RAPID COMMUNICATION | MARCH 29 2011

Communication: The effect of dispersion corrections on the melting temperature of liquid water

Soohaeng Yoo; Sotiris S. Xantheas

J. Chem. Phys. 134, 121105 (2011)
https://doi.org/10.1063/1.3573375

Communication: The effect of dispersion corrections on the melting temperature of liquid water

Soohaeng Yoo and Sotiris S. Xantheas[a)]
Chemical and Materials Sciences Division, Pacific Northwest National Laboratory, 902 Battelle Boulevard, P.O. Box 999, MS K1–83, Richland, Washington 99352, USA

(Received 5 January 2011; accepted 11 March 2011; published online 29 March 2011)

The melting temperature (T_m) of liquid water with the Becke–Lee–Yang–Parr (BLYP) density functional including dispersion corrections (BLYP-D) and the Thole-type, version 3 (TTM3-F) *ab-initio* based flexible, polarizable classical potential is reported via constant pressure and constant enthalpy (*NPH*) molecular dynamics simulations of an ice I_h-liquid coexisting system. Dispersion corrections to BLYP lower T_m to about 360 K, a large improvement over the value of $T_m > 400$ K previously obtained with the original BLYP functional under the same simulation conditions. For TTM3-F, $T_m = 248$ K from classical molecular dynamics simulations. © *2011 American Institute of Physics*. [doi:10.1063/1.3573375]

The simulation of the phase diagram of water[1–6] and especially the melting temperature (T_m) provides information regarding the phase boundary between the solid and liquid phases on the pressure–temperature (P–T) scale. The phase diagram for different approximations of the underlying potential describing the interactions between water molecules, whether this is computed from an electronic structure *ansatz* or an analytical function, represents one of the important benchmarks of the corresponding electronic structure method or the potential function. For example, the TIP4P/2005 (Ref. 3) and TIP4P/Ice (Ref. 4) potentials are regarded as improvements over the original TIP4P potential, since they better reproduce the phase diagram of water. The knowledge of the melting lines of water with various potentials provides useful information about the range of conditions that should be employed in the simulations in order to ensure that the desired phase is described. Our previous study[6] of T_m of Ice I_h with the Perdew–Burke–Ernzerhof (PBE) (Ref. 7) and Becke–Lee–Yang–Parr (BLYP) (Refs. 8 and 9) density functionals produced values of $T_m > 400$ K. These higher values of T_m are consistent with previous reports that those two functionals produced an over-structured liquid not only at room T but also at elevated T up to 400 K (Refs. 10–15) and also that a liquidlike diffusion was reported to occur near an elevated temperature of $T = 400$ K.[16,17]

The higher T_m with these two DFT functionals can be attributed to certain deficiencies in describing the intermolecular interactions between water molecules, such as (but certainly not exclusively due to) the accurate description of the London dispersion interactions.[18–21] To this end, the inclusion of dispersion corrections in the DFT (DFT-D) has been proposed in order to improve the functionals.[19–21] Recently, BLYP-D produced superior results for liquid water when compared to BLYP.[22–24] For example, Born–Oppenheimer molecular dynamics (BOMD) simulations with BLYP-D near ambient conditions yielded[22] a density of ~1 g/cm^3, a pressure of 1 bar, and an oxygen–oxygen radial distribution function (RDF) that is more consistent with the experimental data. The use of dispersion-corrected atom-centered potentials produced RDFs in much better agreement with experiment and a more than three-fold increase in the self-diffusion coefficient.[24] All these are dramatic improvements over the corresponding values of those properties with the original BLYP.

On the other hand, classical, *ab-initio* based potentials for water have risen to the level of sophistication that can accurately describe many of the static, dynamical, and spectral properties of both water clusters and liquid water. For instance, the *ab initio*-based flexible, polarizable Thole-type, version 3 (TTM3-F) potential for water[25–28] has been reported to yield accurate structural, dynamical, transport, and spectral properties of liquid water.[29–34] Since this model was parameterized using the results of high-level *ab initio* calculations of the water dimer potential energy surface[35] and validated from the analysis of the energetics of small water clusters,[36–39] it provides a realistic representation of the full multidimensional BO potential energy surface. Furthermore, since polarization effects are explicitly included in the form, the atomic charges of each water molecule vary instantaneously in response to any structural modification of the local environment.[27] Here, we report the T_m of water with BLYP-D and the TTM3-F potential.

At T_m the chemical potentials of the liquid and ice phases are equal, $\mu_{liq}(P, T_m) = \mu_{ice}(P, T_m)$, and the Gibbs free energy is needed for estimating T_m at a given pressure (P, T_m). The computational approaches for obtaining the free energy are reviewed in Ref. 1. We used a solid–liquid coexisting system in the (*NPH*) ensemble (constant particle number, pressure, and enthalpy) as in our previous studies.[5,40–44] The constant enthalpy (H) constraint results in the solid–liquid system being an isolated one, as it is not allowed to transfer heat from or to the surroundings. When the initial $T < T_m$, the chemical potential of the liquid is higher than that of the ice phase, μ_{liq}

a)Electronic mail: sotiris.xantheas@pnl.gov.

$(P, T) > \mu_{ice}(P, T)$. This results in some molecules of the liquid phase to freeze into ice by simultaneously releasing heat. The released heat results in the increase of the temperature of the system toward T_m. In this respect, MD simulations in the (*NPH*) ensemble for the ice–liquid coexisting system allow for T to be adjusted spontaneously so at $T = T_m$ it satisfies the condition $\mu_{liq}(P, T_m) = \mu_{ice}(P, T_m)$. In preparing the simulation system, an initial proton-disordered ice configuration satisfying the Bernal–Fowler rules with a total dipole moment of zero was constructed, according to the method suggested by Hayward and Reimers.[45]

For the BOMD (*NPH*) simulations with BLYP-D, we used the same initial configuration of the ice–liquid coexisting system as in our previous study[6] with BLYP. We used a coexisting system consisting of 192 water molecules (initially 96 icelike and 96 liquidlike) in a simulation cell of dimensions 13 Å × 15 Å × 28 Å. The simulations were performed using QUICKSTEP,[46] a part of the CP2K program. We adopted the hybrid Gaussian and plane-wave (GPW) method. The core electrons were removed by the introduction of norm-conserving pseudopotentials developed by Goedecker, Teter, and Hutter (GTH) (Refs. 47 and 48) with a charge density cutoff of 280 Ry for the auxiliary basis set. The BLYP exchange-correlation functional[8,9] with the dispersion correction[19,20] (BLYP-D) was used. The Kohn–Sham orbitals were expanded into a triple-ζ valence basis set augmented with two sets of *d*-type or *p*-type polarizable functions (TZV2P). A cutoff radius of 40.0 Å was chosen for the dispersion interaction. A BOMD algorithm was used with a standard velocity Verlet algorithm with a 0.5 fs time step. For the convergence of the wavefunction, we used the criterion $\varepsilon_{SCF} = 1 \times 10^{-7}$ for the electronic gradient with the orbital transformation method.

For the simulations with the TTM3-F (Ref. 28) potential, the ice–liquid coexisting system consists of 1536 water molecules (initially 768 icelike and 768 liquidlike) in a simulation cell of dimensions 27 Å × 31 Å × 58.5 Å. The detailed approach to set up the initial coexisting system has been previously discussed.[5,6,42] The van der Waals interactions within a sphere of $R = 10.0$ Å were considered for each atom, while standard long-range corrections for the energy and pressure were applied. For the electrostatic interactions, the radius of the sphere was 10.0 Å, while the Ewald summation technique was adopted.[49] The velocity Verlet algorithm[50] was used to propagate the trajectory with a 1 fs time step.

For the BLYP-D functional, the instantaneous kinetic temperature T versus the MD simulation time t from two independent systems with initial temperatures of $T = 350$ and 370 K is shown in Fig. 1. The kinetic temperatures of the two systems gradually converge to $T_m = 360 \pm 2$ K, a value that is ~50 K lower than the corresponding one with BLYP (without dispersion corrections) under the same simulation protocol. The reported error bar was estimated as follows: after the initial 8 ps of simulation (cf. Fig. 1), the next 5 ps were used to estimate the error bar based on the standard deviation (see the additional discussion in the conclusions paragraph about the error bar). In addition to T_m, the pressure at $\rho = 1$ g/cm^3 is also improved from 10 000 bar (BLYP) to 1 bar (BLYP-D).[22] Therefore, the BLYP-D functional, besides a more accurate value for the density, the pressure, and the RDF of water near ambient conditions,[22] also produces a more accurate value for T_m when compared to BLYP.

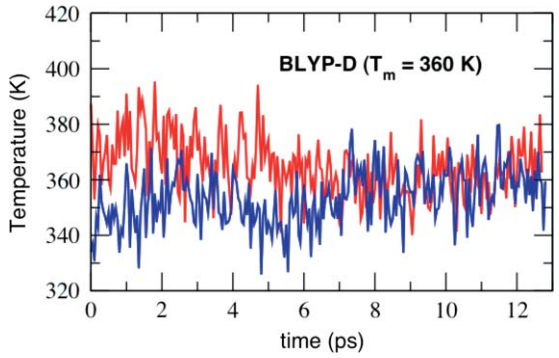

FIG. 1. The coexisting ice I_h-liquid classical simulation in the (*NPH*) ensemble at $P = 1$ bar with the BLYP-D (BLYP + Dispersion) functional for $\rho = 1$ g/cm^3.

Figure 2 shows the comparison of the oxygen–oxygen RDFs from (*NVT*) classical simulations of a supercell of 125 water molecules at $\rho = 1$ g/cm^3 for the BLYP (red) and BLYP-D (blue). The dashed line corresponds to the experimental RDF. Instead of comparing the RDFs of different models at the same T, we have instead chosen to use a relative-to T_m temperature scale for each case.[34] The comparison is made at $T = T_m + 25$ K, viz., at $T = 436$ K (BLYP), $T = 385$ K (BLYP-D), and $T = 298$ K (experiment). Overall, we find that liquid water with BLYP is severely understructured with respect to experiment at the same relative (with respect to T_m) scale, as evidenced from the heights of the first and second peaks and the fact that the first minimum is too shallow. The dispersion correction produces a higher first peak that is closer to experiment than BLYP albeit it is practically identical to (or slightly worst than) BLYP for $R > 3.5$ Å. Our results are consistent with recent findings[22] that at $T = 330$ K BLYP-D produces a first peak that is quite close to the experimental one at ambient temperature, i.e., is more structured than the higher temperature ($T = 385$ K) reported here.

Figure 3 shows the comparison between the mean square displacements (MSD) for BLYP and BLYP-D at the

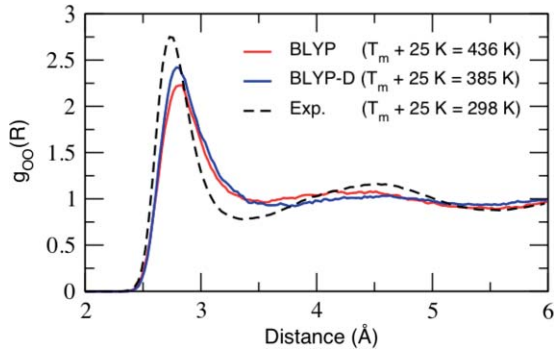

FIG. 2. Comparison of the oxygen–oxygen RDFs from (*NVT*) classical simulations of a supercell of 125 water molecules for $\rho = 1$ g/cm^3 at $T = T_m + 25$ K between the BLYP (red) and BLYP-D (blue) functionals. The dashed line corresponds to the experimental oxygen–oxygen RDF. Note that the comparison is performed at *different* absolute temperatures for each case since T_m (BLYP) = 411 K, T_m (BLYP-D) = 360 K and T_m (expt.) = 273 K.

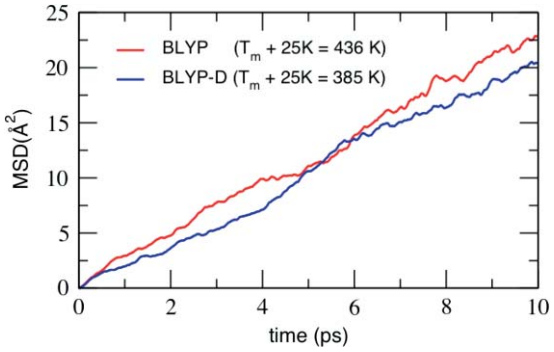

FIG. 3. Comparison of the mean square displacements from (*NVT*) classical simulations of a supercell of 125 water molecules for $\rho = 1$ g/cm^3 at $T = T_m + 25$ K for the BLYP (red) and BLYP-D (blue) potentials. Note that the comparison is performed at *different* absolute temperatures for each case since T_m (BLYP) = 411 K, T_m (BLYP-D) = 360 K.

$T = T_m + 25$ K relative temperatures. The diffusion constant (D) is obtained from the MSD via

$$D = \frac{\text{MSD}}{6t} = \lim_{t\to\infty} \frac{1}{6} \left\langle \frac{1}{N} \sum_i |r_i(t) - r_i(0)|^2 \right\rangle. \quad (1)$$

The MSDs were computed from the relative displacements of the oxygen atoms and averaged over all water molecules and all configurations of the full trajectory.[51] The MSDs are almost identical for those two relative T's for the two functionals. Figures 2 and 3 suggest that the results with the two different functionals exhibit similar RDFs and MSDs when placed at the same thermodynamic conditions (i.e., at $T = T_m + 25$ K).

Figure 4 shows the instantaneous kinetic temperature T vs t for the two initial temperatures of $T = 250$ and 255 K with the TTM3-F potential. The two different initial kinetic temperatures slowly merge into the value of $T_m \sim 248 \pm 2.5$ K. The data after 200 ps were used for calculating the average of T_m and the estimation of the error bar. The later was estimated from the standard deviation of T averaged every 20 ps. A previous study[31] has yielded $T_m = 242.5 \pm 1.5$ K for version 2.1 of the Thole-type model (TTM2.1-F) (Ref. 27) as a result of classical (*NPT*) MD simulations with the ice–liquid coexisting system. When compared to the results with the TTM2.1-F potential, the T_m of TTM3-F was found to be higher by ~5.5 K. It is expected that the inclusion of quantum effects will result in lowering T_m as was previously shown for the TTM2.1-F potential.[29]

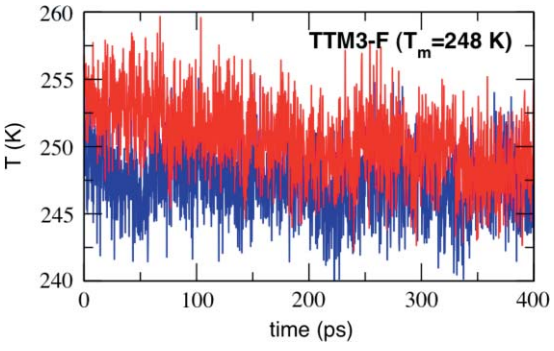

FIG. 4. The coexisting ice I_h-liquid classical simulation in the (*NPH*) ensemble at $P = 1$ bar with the *ab-initio* based flexible, polarizable TTM3-F potential at $\rho = 1$ g/cm^3.

In summary, the melting temperatures with the BLYP-D density functional and the TTM3-F *ab-initio* based classical potential were estimated using the ice–liquid coexisting system via simulations in the constant pressure and constant enthalpy (*NPH*) ensemble. We obtained $T_m = 360$ K at $P = 1$ bar (BLYP-D) and $T_m = 248$ K at $P = 1$ bar (TTM3-F). The uncertainty of T_m with the BLYP-D functional reported earlier in this paper (± 2 K) is probably too optimistic for a simulation of a few ps. In this respect, it can be viewed as a rough idea of T_m being close to 360 K with a more realistic uncertainty perhaps as high as 10 K. However, as this equally applies to the simulation with the original BLYP reported earlier, the gross effect that the dispersion has in lowering T_m by ~50 K remains unchanged.

The success of dispersion corrections added to standard density functionals in describing better several macroscopic properties of liquid water, including the melting temperature, is promising for the further development of more accurate functionals to describe aqueous environments. The present study furthermore establishes the range of appropriate conditions that should be used in conjunction with those functionals and/or classical potentials to ensure that a liquid phase is described in the simulations.

Work supported by the Division of Chemical Sciences, Geosciences and Biosciences, Office of Basic Sciences, (U.S.) Department of Energy (DOE). Battelle operates the Pacific Northwest National Laboratory for the DOE. This research was performed in part using the Molecular Science Computing Facility in the Environmental Molecular Sciences Laboratory, a national scientific user facility sponsored by the DOE's Office of Biological and Environmental Research. Additional computer resources were provided by the Office of Basic Energy Sciences at the National Energy Research Scientific Computing Center, a DOE's Office of Science user facility at Lawrence Berkeley National Laboratory.

[1] C. Vega, E. Sanz, J. L. F. Abascal, and E. G. Noya, J. Phys.: Condens. Matter **20**, 153101 (2008).
[2] G. T. Gao, X. C. Zeng, and H. Tanaka, J. Chem. Phys. **112**, 8534 (2000).
[3] J. L. F. Abascal and C. Vega, J. Chem. Phys. **123**, 234505 (2005).
[4] J. L. F. Abascal, E. Sanz, R. G. Fernández, and C. Vega, J. Chem. Phys. **122**, 234511 (2005).
[5] J. Wang, S. Yoo, J. Bai, J. R. Morris, and X. C. Zeng, J. Chem. Phys. **123**, 36101 (2005).
[6] S. Yoo, X. C. Zeng, and S. S. Xantheas, J. Chem. Phys. **130**, 221102 (2009).
[7] J. P. Perdew, K. Burke, and M. Ernzerhof, Phys. Rev. Lett. **77**, 3865 (1996).
[8] A. D. Becke, Phys. Rev. A **38**, 3098 (1988).
[9] C. Lee, W. Yang, and R. G. Parr, Phys. Rev. B **37**, 785 (1988).
[10] J. C. Grossman, E. Schwegler, E. W. Draeger, F. Gygi, and G. Galli, J. Chem. Phys. **120**, 300 (2004).
[11] M. J. McGrath, J. I. Siepmann, I.-F. W. Kuo, C. J. Mundy, J. VandeVondele, J. Hutter, F. Mohamed, and M. Krack, Chem. Phys. Chem. **6**, 1894 (2005).
[12] S. Sastry and A. C. Angell, Nature Mater. **2**, 739 (2003).
[13] O. Mishima and H. E. Stanley, Nature (London) **396**, 329 (1998).
[14] Y. Katayama, T. Mizutani, W. Utsumi, O. Shimomura, M. Yamakata, and K. Funakoshi, Nature (London) **403** (6766), 170 (2000).
[15] I. Brovchenko, A. Geige, and A. Oleinikova, J. Chem. Phys. **123**, 044515 (2005).

[16]E. Schwegler, J. C. Grossman, F. Gyg, and G. Galli, J. Chem. Phys. **121** (11), 5400 (2004).
[17]P. H.-L. Sit and N. Marzari, J. Chem. Phys. **122**, 204510 (2005).
[18]U. Zimmerli, M. Parrinello, and P. Koumoutsakos, J. Chem. Phys. **120**, 2693 (2004).
[19]S. Grimme, J. Comput. Chem. **25**, 1463 (2004).
[20]S. Grimme, J. Comput. Chem. **27**, 1787 (2006).
[21]S. Grimme, J. Antony, S. Ehrlich, and H. Krieg, J. Chem. Phys. **132**, 154104 (2010).
[22]J. Schmidt, J. VandeVondele, I. F. W. Kuo, D. Sebastiani, J. I. Siepmann, J. Hutter, and C. J. Mundy, J. Phys. Chem. B **113**, 11959 (2009).
[23]I. C. Lin and U. Rothlisberger, Chimia **62**, 231 (2008).
[24]I. C. Lin, A. P. Seitsonen, M. D. Coutinho-Neto, I. Tavernelli, and U. Rothlisberger, J. Phys. Chem. B **113**, 1127 (2009).
[25]C. J. Burnham, J. Li, S. S. Xantheas, and M. Leslie, J. Chem. Phys. **110**, 4566 (1999).
[26]C. J. Burnham and S. S. Xantheas, J. Chem. Phys. **116**, 1479 (2002).
[27]G. S. Fanourgakis and S. S. Xantheas, J. Phys. Chem. A **110**, 4100 (2006).
[28]G. S. Fanourgakis and S. S. Xantheas, J. Chem. Phys. **128**, 074506 (2008).
[29]F. Paesani, S. Iuchi, and G. A. Voth, J. Chem. Phys. **127**, 074506 (2007).
[30]S. Habershon, G. S. Fanourgakis, and D. E. Manolopoulos, J. Chem. Phys. **129**, 074501 (2008).
[31]F. Paesani and G. A. Voth, J. Phys. Chem. C **112**, 324 (2008).
[32]F. Paesani and G. A. Voth, J. Phys. Chem. B **113**, 5702 (2009).
[33]F. Paesani, S. S. Xantheas, and G. A. Voth, J. Phys. Chem. B **113**, 13118 (2009).
[34]F. Paesani, S. Yoo, H. J. Bakker, and S. S. Xantheas, J. Phys. Chem. Lett. **1**, 2316 (2010).
[35]C. J. Burnham and S. S. Xantheas, J. Chem. Phys. **116**, 1479 (2002).
[36]S. S. Xantheas, C. J. Burnham, and R. J. Harrison, J. Chem. Phys. **116**, 1493 (2002).
[37]G. S. Fanourgakis, E. Apra, and S. S. Xantheas, J. Chem. Phys. **121**, 2655 (2004).
[38]S. Bulusu, S. Yoo, E. Aprà, S. Xantheas, and X. C. Zeng, J. Phys. Chem. A **110**, 11781 (2006).
[39]A. Lagutschenkov, G. S. Fanourgakis, G. Niedner-Schatteburg, and S. S. Xantheas, J. Chem. Phys. **122**, 194340 (2005).
[40]U. Landman, W. D. Luedtke, R. N. Barnett, C. L. Cleveland, M. W. Ribarsky, E. Arnold, S. Ramesh, H. Baumgart, A. Martinez, and B. Khan, Phys. Rev. Lett. **56**, 155 (1986).
[41]J. R. Morris, C. Z. Wang, K. M. Ho, and C. T. Chan, Phys. Rev. B **49**, 3109 (1994).
[42]S. Yoo, X. C. Zeng, and J. R. Morris, J. Chem. Phys. **120**, 1654 (2004).
[43]R. G. Fernández, J. L. F. Abascal, and C. Vega, J. Chem. Phys. **124**, 144506 (2006).
[44]J. L. F. Abascal, R. G. Fernández, C. Vega, and M. A. Carignano, J. Chem. Phys. **125**, 166101 (2006).
[45]J. A. Hayward and J. R. Reimers, J. Chem. Phys. **106**, 1518 (1997).
[46]J. VandeVondele, M. Krack, F. Mohamed, M. Parrinello, T. Chassaing, and J. Hutter, Comp. Phys. Comm. **167**, 103 (2005).
[47]S. Goedecker, M. Teter, and J. Hutter, Phys. Rev. B **54**, 1703 (1996).
[48]C. Hartwigsen, S. Goedecker, and J. Hutter, Phys. Rev. B **58**, 3641 (1998).
[49]T. M. Nymand and P. Linse, J. Chem. Phys. **112**, 6152 (2000).
[50]W. C. Swope, H. C. Andersen, P. H. Berens, and K. R. Wilson, J. Chem. Phys. **76**, 637 (1982).
[51]D. Frenkel and B. Smit, *Understanding Molecular Simulation From Algorithms to Applications* (Academic, San Diego, 2001).